

RESEARCH

Open Access



# The diverse functions of *Pseudomonas syringae syringae* van Hall effectors in regulating the plant immune response

Xiang Wang<sup>1†</sup>, Fei Yan<sup>1†</sup>, Guojing Ma<sup>1</sup>, Aixia Li<sup>1</sup> and Lijing Liu<sup>1\*</sup> 

## Abstract

Sorghum relies on its immune system to defend against various pathogens, including *Pseudomonas syringae syringae* van Hall (*Pss* van Hall). However, the sorghum immune system is largely unknown. Reports on pathogenic effectors have provided valuable insights into the plant immune system; thus, we aimed to identify *Pss* van Hall effectors that can regulate the sorghum defense response in this study. Here, we first established the sorghum-*Pss* van Hall pathosystem and found that type III effectors played critical roles in the virulence of *Pss* van Hall to sorghum. To predict its effectors, the whole genome of *Pss* van Hall was sequenced, and 18 effector-coding genes were identified. Among them, five effectors belong to the core effectors of *Pseudomonas syringae* pathovars, and two may be monocot pathogen-specific effectors. *Pss* van Hall triggered the hypersensitive response (HR) in *Nicotiana benthamiana*. We found that the effectors of *Pss* van Hall can be divided into cell death inducers and immune repressors by examining their functions in HR induction and repression of PTI marker gene, ROS production, and pathogen growth. Finally, the roles of core effectors HopAJ2 and HopAN1, and specific effector HopAX1 were further confirmed in the sorghum-*Pss* van Hall pathosystem. Importantly, the functions of HopAN1 and HopAX1 in regulating plant immunity were reported for the first time. We believe that the identification of these effectors will facilitate the continued exploration of the sorghum immune system.

**Keywords** Sorghum, Effectors, *Pseudomonas syringae syringae*, PTI, Hypersensitive response

## Background

Sorghum [*Sorghum bicolor* (L.) Moench] is among the top five cereal crops that serves as a major source of food for millions of people worldwide (Khoddami et al. 2021). In addition, sorghum is also a valuable source of fiber, forage, and fuel (Rooney et al. 2007; Colombini et al. 2012). In 2009, the first sorghum genome sequence was

published, and the small diploid genome (approximately 730 Mb) makes it an ideal model for studying C4 crops (Paterson et al. 2009; Calvino and Messing 2012). Since it was domesticated in central eastern Sudan with arid and semiarid ecosystems (Dillon et al. 2007), sorghum is a versatile crop that can adapt to many abiotic stresses, such as drought, salt, and alkalinity, making it an ideal crop for many regions to ensure food security (Xie and Xu 2019; Ma et al. 2020; Prasad et al. 2021). However, sorghum still faces a serious threat from various diseases that affect its growth and productivity, leading to significant economic losses for farmers (Ackerman et al. 2021; Mewa et al. 2022; Sun et al. 2022). Therefore, there is a growing need to explore the sorghum immune system to

<sup>†</sup>Xiang Wang and Fei Yan have contributed equally to this work

\*Correspondence:

Lijing Liu  
ljliu@sdu.edu.cn

<sup>1</sup>The Key Laboratory of Plant Development and Environmental Adaptation Biology, Ministry of Education, School of Life Sciences, Shandong University, Qingdao 266237, China



promote its disease resistance ability through molecular strategies.

Sorghum leaf spot disease is the result of a bacterial infection caused by *Pseudomonas syringae syringae* van Hall (*Pss* van Hall) (Anitha et al. 2020). This disease is characterized by initially small, circular lesions on the leaves of the sorghum plant and then irregularly shaped with a straw color center and dark margin, sometimes even resulting in death of the whole leaf. *Pss* van Hall can cause significant damage to plant foliage, ultimately resulting in reduced yield and quality of the crop. However, the virulence determinants of *Pss* van Hall in sorghum are still unknown. *Pss* van Hall is a member of the *Pseudomonas syringae*, which includes many species that can cause significant damage to a wide range of plants, including vegetables, fruits, and trees (Ivanovic et al. 2017; Donati et al. 2018; Xin et al. 2018). In addition, the Arabidopsis-*Pseudomonas syringae* pathosystem has been used as a model for exploring the general knowledge of the plant immune system in the last 30 years (Quirino and Bent 2003; Xin and He 2013).

Based on studies on the Arabidopsis-*Pseudomonas syringae* pathosystem, the plant innate immune system is divided into two major branches: pattern-triggered immunity (PTI) and effector-triggered immunity (ETI) (Jones and Dangl 2006; Ngou et al. 2022). PTI is a first line of defense mechanism that is triggered when plants encounter pathogen-associated molecular patterns (PAMPs), which are conserved molecules derived from pathogens (Kunze et al. 2004; Chinchilla et al. 2006). When PAMPs are detected by pattern recognition receptors (PRRs) on plant cell surfaces, they activate a cascade of signaling pathways to restrict the invasion or proliferation of pathogens. Pathogens, such as *P. syringae* pv. *tomato* (*Pst*) DC3000, can secrete effectors into plant cells to manipulate plant cellular processes and suppress PTI, which results in successful infection (Clark et al. 2018; Todd et al. 2022). This phenomenon is called effector-triggered susceptibility (ETS), and ETS-induced effectors are named virulent effectors. Some effectors or their activities can be recognized by intracellular nucleotide-binding domain leucine-rich repeat-containing receptors (NLRs), leading to a more specific and robust defense mechanism termed ETI, which is generally associated with the hypersensitive response (HR) and restriction of pathogen growth (Kunkel et al. 1993; Gassmann and Bhattacharjee 2012). The effectors that induce ETI are called avirulent effectors (White et al. 2000; Qi et al. 2022). Due to the roles of effectors in triggering ETS and ETI, their studies have helped us to explore knowledge about the plant immune system. However, the effectors triggering sorghum ETS and ETI, to the best of our knowledge, have not been explored.

In this study, we predicted 18 effectors from *Pss* van Hall by sequencing its whole genome. Among them, five effectors belong to the core effectors of *P. syringae* pathovars, and two may be monocot pathogen-specific effectors. The *Pss* van Hall effectors can be divided into virulent and avirulent effectors depending on their influences on the immune system of *Nicotiana benthamiana*, and the functions of core effectors HopAJ2 and HopAN1, and specific effector HopAX1 were further confirmed in the sorghum-*Pss* van Hall pathosystem. Collectively, our study, for the first time, reported effectors that can regulate the pathogenicity of *Pss* van Hall in sorghum, which will be good tools to understand the sorghum immune system in the future.

## Results

### Type III effectors are critical for the pathogenicity of *Pss* van Hall in sorghum

As there is no report on the sorghum infection conditions for *Pss* van Hall, we first built the sorghum-*Pss* van Hall pathosystem and found that *Pss* van Hall can produce severe disease lesions on the leaves of sorghum under our conditions (Additional file 1: Figure S1a). The propagation of *Pss* van Hall in sorghum was further quantified by analyzing the DNA level of its *Histone* gene with that of the *SbEIF4A* gene as a control. As shown in Additional file 1: Figure S1b, the relative expression level of *Histone* was approximately 75-fold higher than that of *SbEIF4A* in the *Pss* van Hall-infected samples, while no *Histone* DNA was detected in the control (buffer inoculated) sample. Moreover, *Pss* van Hall triggered HR on leaves of *N. benthamiana* within two days after infiltration (Additional file 1: Figure S1c). We further measured the cell death using an ion leakage assay (Liu et al. 2016). Consistent with the HR phenotype, more cell death was observed in *Pss* van Hall infiltrated leaves (Additional file 1: Figure S1d).

As type III effectors, secreted through the type III secretion system (T3SS), have been shown to be required for the successful infection of *P. syringae* pathovars (Tang et al. 2006; Wei et al. 2018), we wondered whether type III effectors are also critical for the pathogenicity of *Pss* van Hall. To test this hypothesis, we mutated the *hrpL* gene of *Pss* van Hall, which is a critical factor in regulating the expression of T3SS (Tang et al. 2006), using homologous recombination. Based on previous results on other pathogens of *Pseudomonas*, T3SS is unable to function normally without HrpL. Compared with the wild-type strain,  $\Delta hrpL$  had significantly reduced pathogenicity in sorghum, as indicated by the almost complete loss of disease lesions on the sorghum leaves (Fig. 1a). The statistical analysis of the pathogen biomass also showed that  $\Delta hrpL$  greatly reduced the reproductive

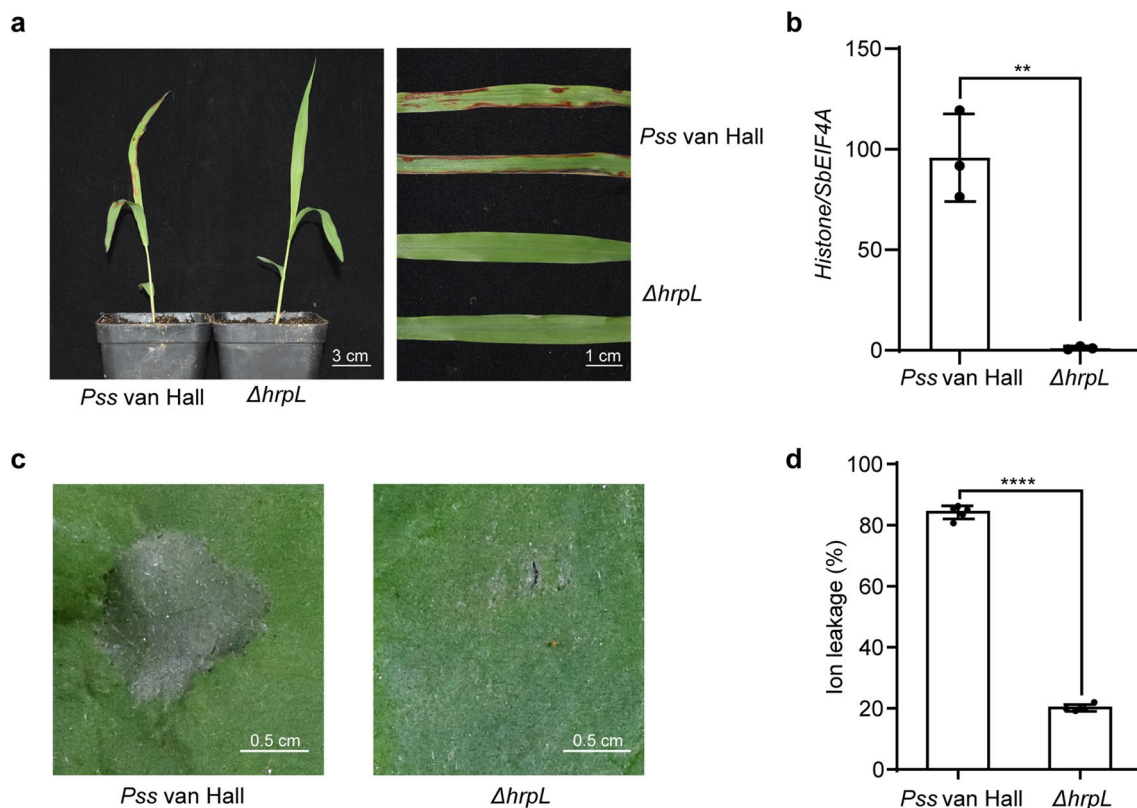


**Fig. 1** Type III effectors play critical roles in the pathogenic infection of *Pss van Hall* in sorghum. **a** Representative seedling and leaves of sorghum infected with *Pss van Hall*. Two-week-old sorghum plants were treated with *Pss van Hall* or the  $\Delta hrpL$  strain for 2 days at 12 °C and then kept at 25 °C for an additional 3 days. **b** The DNA level of the pathogen *Histone* gene, which is normalized to the DNA level of the sorghum gene *SbEIF4A*. Data are shown as the mean  $\pm$  SD ( $n=3$ ). **c** Representative *N. benthamiana* leaf infected with *Pss van Hall* or the  $\Delta hrpL$  strain. Leaves from five-week-old *N. benthamiana* were infiltrated with *Pss van Hall* or the  $\Delta hrpL$  strain for 2 days at 25 °C. **d** Conductivity measurement of *Pss van Hall*- or  $\Delta hrpL$ -infiltrated *N. benthamiana* leaves. Data are shown as the mean  $\pm$  SD ( $n=5$ ). All experiments were repeated three times with similar results. Significant differences were detected using Student's *t* test. \*\*  $p < 0.01$ ; \*\*\*\*  $p < 0.0001$

ability of *Pss van Hall* in sorghum (Fig. 1b). Additionally, the  $\Delta hrpL$  mutant strain cannot induce HR on leaves of *N. benthamiana* (Fig. 1c, d). These results suggest that the T3SS is essential for the pathogenicity of *Pss van Hall* in sorghum and the induction of HR in *N. benthamiana*.

#### The prediction of *Pss van Hall* type III effectors via genome sequencing

For the purpose of exploring effectors of *Pss van Hall*, we used Illumina HiSeq combined with third-generation sequencing technologies to sequence its genome. A total of 12,754,663 reads with an average sequencing depth of over 600 times were generated by sequencing (Fig. 2a). Based on the sequencing results, the *Pss van Hall* strain contains one circular chromosome with a length of 6.15 Mb. This chromosome contains a total of 4091 coding sequences (CDS), which covered 68.00% of the entire genome. Additionally, there were found to contain 70 tRNA and 17 rRNA genes (Fig. 2a). Then, we visualized the *Pss van Hall* chromosome using CGView to show

the distributions of coding genes, tRNA, and rRNA and changes in genomic GC content and GC bias (Stothard et al. 2019). The visualization results showed that the coding regions of the *Pss van Hall* genome were evenly distributed throughout the entire genome and that the GC content within the genome intervals was generally stable (Fig. 2b). KEGG (Kyoto Encyclopedia of Genes and Genomes) analysis was performed to show the functions of proteins encoded by CDSs in the *Pss van Hall* genome, and we found that they were enriched in processes such as ABC transporters, biosynthesis of amino acids, and carbon metabolism (Fig. 2c).

A total of 18 type III effector-encoding genes were predicted using the effector sequences of other pathogenic variants of *Pseudomonas syringae* as probes to blast the *Pss van Hall* genome (Additional file 2: Table S1) (Ravindran et al. 2015). The protein size of these effectors vary from 11 to 179 kD, with AvrE being the largest and HopJ being the smallest (Additional file 2: Table S1). Among these effectors, AvrE,

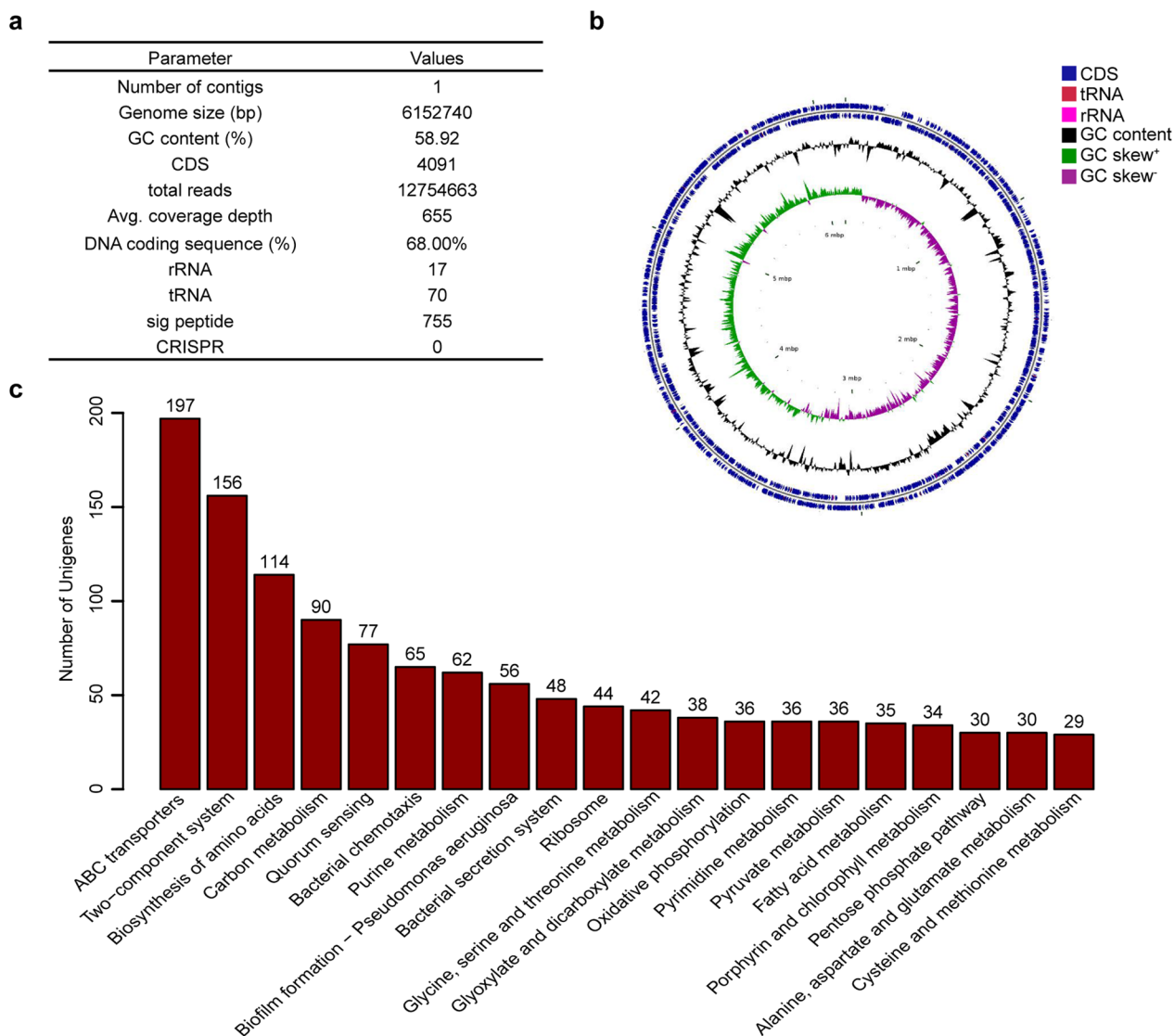


**Fig. 2** The genome information of *Pss* van Hall. **a** General features of *Pss* van Hall are presented. **b** The *Pss* van Hall chromosome was visualized using CGView, with the innermost circle displaying the genome sequence position. Moving outward, the circles represent the GC skew, GC content, and predicted coding genes (CDS, tRNA, and rRNA). **c** KEGG analysis was performed to reveal the functions of proteins encoded by CDSs in the *Pss* van Hall genome. The number above each column represents the protein number in the corresponding process

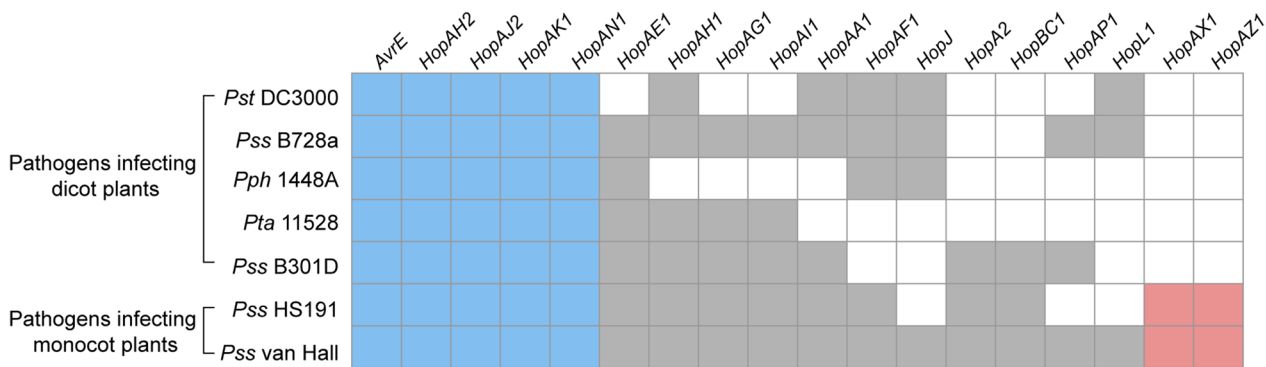


**Fig. 3** Distribution of effectors in different *P. syringae* pathovars. Gray boxes indicate the presence of type III effectors in the analyzed strain. Blue boxes represent conserved core effectors. Red boxes represent type III effectors that are specific to pathogens that infect monocot plants

HopAH2, HopAJ2, HopAK1, and HopAN1 are conserved core effectors, as they also exist in all six previously sequenced *P. syringae* pathovars, including *Pst* DC3000, *Pss* B728a, *P. syringae phaseolicola* 1448A, *P. syringae tabaci* 11528, *Pss* B301D, and *Pss* HS191 (Fig. 3) (Studholme et al. 2009; Ravindran et al. 2015). HopAZ1 and HopAX1 are effectors specifically in monocot plant infection pathogens, *Pss* van Hall and *Pss* HS191 (Fig. 3), indicating that these specific effectors may play critical roles in the interactions of *P. syringae* with monocot plants.

#### Diverse roles of *Pss* van Hall effectors in defense regulation in *N. benthamiana*

To investigate the contribution of individual *Pss* van Hall effectors to pathogenicity, we cloned the CDSs of all 18 effectors using PCR (Additional file 1: Figure S2) and conjugated them into pPSE, a *Pseudomonas*-expressing vector constructed in this study (Additional file 1: Figure S3a). The pPSE vector harbors a GFP expression cassette, and a clear GFP signal can be observed after transfer into *Pst* DC3000 D36E and *Pss* van Hall (Additional file 1: Figure S3b, c) (Wei et al. 2018). To verify the effective expression and translocation of effectors using pPSE, we replaced the coding sequence of *GFP* with *HrpZ* and *AvrRpt2* and then transformed the final constructs into the *Pst* DC3000 D36E strain. The expression of *HrpZ* and *AvrRpt2* induced HR in *N. benthamiana* and *Arabidopsis*, respectively, as expected (Additional file 1: Figure S3d, e) (Kunkel et al. 1993; Alfano et al. 1996).

To avoid functional redundancy among effectors in studying their interactions with plants, we transformed the constructs of *Pss* van Hall effectors into the *Pst* DC3000 D36E strain, which has all 36 effectors of *Pst* DC3000 deleted (Wei et al. 2018). All *Pss* van Hall effectors could be well expressed in *Pst* DC3000 D36E (Additional file 1: Figure S4). To verify whether these effectors could be secreted into the host cell, we conjugated a C-terminal calmodulin-dependent adenylate cyclase (*Cya*) tag to the effectors (Matas et al. 2014). As shown in Fig. 4a, all 18 effectors of *Pss* van Hall were successfully delivered into plant cells at 6-h post infection.

As *Pss* van Hall triggered HR in *N. benthamiana*, we first examined which effectors are responsible for this phenomenon. The *Pst* DC3000 D36E strains carrying various *Pss* van Hall effectors were infiltrated into leaves of *N. benthamiana* for two days to trigger HR. As shown in Fig. 4b, HopAA1, HopAJ2, HopAN1, and HopJ, but not GFP control and other effectors, caused clear HR on leaves of *N. benthamiana*. Compared with the GFP control, samples infiltrated with HopAA1, HopAJ2, HopAN1, and HopJ showed accumulated ion leakage (Fig. 4c). These results prove that HopAA1, HopAN1, HopAJ2, and HopJ of *Pss* van Hall have the capability to induce cell death in *N. benthamiana*.

*Pst* DC3000 D36E could induce PTI in *N. benthamiana*, including the upregulation of well-known PTI marker genes, such as *Pti5* and *ACRE31* and ROS elicitation (Cong et al. 2023). Then, we further checked if any *Pss* van Hall effectors could inhibit the activation of these genes. Samples were collected six hours after pathogen infiltration into leaves of *N. benthamiana*. As expected, the strains transformed with GFP control highly induced the expression of these marker genes compared to the buffer infiltrated sample (CK). Among all 18 *Pss* van Hall effectors, *AvrE*, HopAA1, HopAF1, HopAH2, HopAJ2, HopAK1, HopAN1, and HopAP1 did not repress the activation of any PTI marker genes; HopA2 and HopJ showed weak repression of the expression of one PTI marker gene (Fig. 5a, b). The remaining effectors, HopAE1, HopAG1, HopAH1, HopAI1, HopAX1, HopAZ1, HopBC1, and HopL1, inhibited the upregulation of both PTI-related marker genes (Fig. 5a, b).

We then investigated whether the effectors were able to suppress ROS production during infection and found all 18 *Pss* van Hall effectors, except HopAI1 and HopL1, could inhibit the ROS production (Fig. 5c). To further explore the roles of *Pss* van Hall effectors in its pathogenicity, we examined the pathogen accumulation in the leaves of *N. benthamiana*. As shown in Fig. 5d, 12 of these effectors, including *AvrE*, HopA2, HopAE1, HopAF1, HopAG1, HopAH1, HopAK1, HopAP1, HopAX1, HopAZ1, HopBC1, and HopL1, could enhance, while HopAJ2 and HopAN1 could repress, the pathogenicity

(See figure on next page.)

**Fig. 4** Identification of *Pss* van Hall effectors that induce HR in *N. benthamiana*. **a** Leaves of five-week-old *N. benthamiana* were infiltrated with *Pst* DC3000 D36E harboring the pPSE vector with *Cya* (vector) or different *Pss* van Hall effectors conjugated with *Cya*. Six hours later, samples were collected for cAMP assay. Data are shown as the mean  $\pm$  SD ( $n=3$ ). **b** Representative *N. benthamiana* leaf infected with *Pst* DC3000 D36E harboring the pPSE vector (GFP) or pPSE with different *Pss* van Hall effectors. Leaves from five-week-old *N. benthamiana* were infiltrated with *Pst* DC3000 D36E harboring the pPSE vector (GFP) or pPSE with different *Pss* van Hall effectors for 2 days at 25 °C. Bar = 0.5 cm. **c** Conductivity measurement of *N. benthamiana* leaves infiltrated with *Pst* DC3000 D36E harboring the pPSE vector (GFP) or pPSE with different *Pss* van Hall effectors. Data are shown as the mean  $\pm$  SD ( $n=5$ ). All experiments were repeated three times with similar results. Significant differences were detected using Student's *t* test. \*  $p < 0.05$ ; \*\*  $p < 0.01$ ; \*\*\*  $p < 0.001$ ; \*\*\*\*  $p < 0.0001$

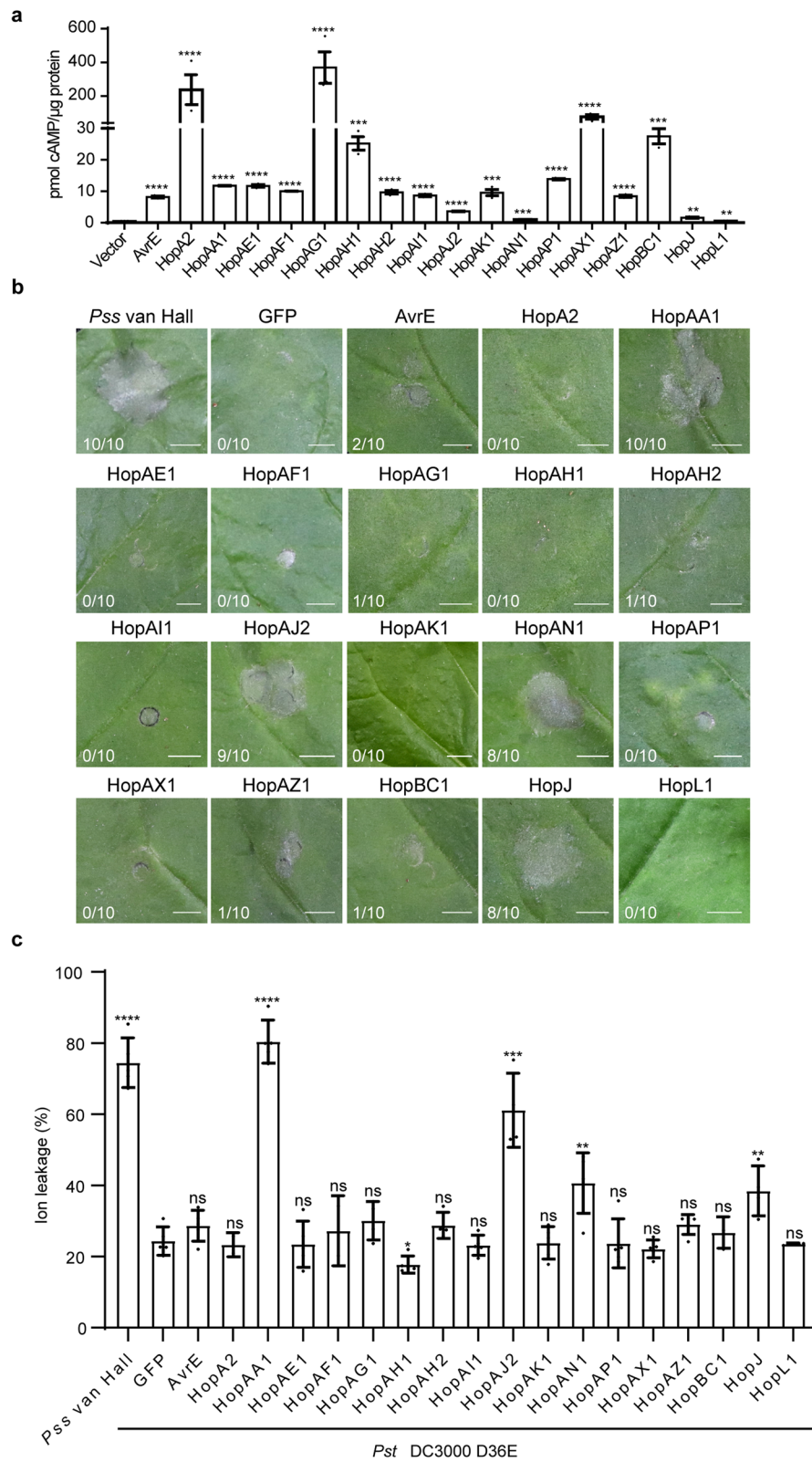


**Fig. 4** (See legend on previous page.)

of *Pst* DC3000 D36E in *N. benthamiana*. Among them, HopAE1, HopAG1, HopAH1, HopAX1, HopAZ1, and HopBC1 showed consistent results in the inhibition of PTI marker gene's expression, ROS production and pathogen growth, indicating they are the key effectors to suppress PTI.

#### The functions of the *Pss* van Hall core and specific effectors in the sorghum immune response

In the above experiments in *N. benthamiana*, we observed an interesting phenomenon: the *Pss* van Hall core effectors HopAJ2 and HopAN1 can elicit cell death and the specific effectors HopAX1 and HopAZ1 are PTI inhibition effectors. We hypothesized that sorghum encodes some conserved NB-LRR proteins, which exist in both sorghum and *N. benthamiana*, to recognize the core effectors to prevent *Pss* van Hall infection, while *Pss* van Hall has also evolved new effectors to repress defense for successful invasion. To test this hypothesis, we overexpressed HopAJ2, HopAN1, HopAX1, and HopAZ1 in *Pss* van Hall (Additional file 1: Figure S5) and found that the overexpression of these effectors did not restrict the growth of *Pss* van Hall in KB medium (Additional file 1: Figure S6). The obtained transformants with HopAJ2 and HopAN1 were first used to infect sorghum plants to monitor whether they can induce HR in sorghum. However, we did not observe visible HR after infection (Fig. 6a), suggesting that these two effectors are not HR-inducer or their functions might be repressed by other effectors of *Pss* van Hall in sorghum. Lesions caused by infection with HopAJ2 and HopAN1 overexpression strains were significantly fewer in sorghum leaves compared with those infected with the control strain, and surprisingly, HopAN1 overexpression almost blocked the formation of lesions (Fig. 6a). This phenomenon is consistent with the pathogen growth inhibition function of ETI. Further qPCR analysis was performed, and less pathogen DNA was detected in samples infected with HopAJ2- and HopAN1-overexpression strains than in control-treated samples (Fig. 6b). These results prove that the *Pss* van Hall core effectors HopAJ2 and HopAN1, even cannot induce HR, could still be recognized by plants to restrict pathogen infection in sorghum.

Then, we infected sorghum with transformants of HopAX1 and HopAZ1 to examine whether they could repress sorghum immunity. As shown in Fig. 7a, overexpressing HopAX1 in *Pss* van Hall resulted in more severe formation of lesions in sorghum leaves compared with the vector control. However, increasing the expression of HopAZ1 reduced the formation of lesions (Fig. 7a), indicating that the HopAZ1 involved in eliciting sorghum immune response. These results were confirmed by qPCR to monitor pathogen growth in plants (Fig. 7b). Collectively, our data identified an immune repressor, HopAX1, in the interaction of *Pss* van Hall and sorghum.

#### Discussion

Sorghum is a versatile crop used for food, livestock feed, and bioenergy materials. However, its growth and yield have been limited by infectious diseases, compounded by the effects of climate change (Anitha et al. 2020; Mewa et al. 2022). In recent years, multiple efforts have been made to understand the sorghum immune response and identify defense-related genes. Similar to other plant species, sorghum likely employs PTI and ETI as the key immune responses, even though most components of these signaling pathways have yet to be explored. Previous studies have shown that flg22, a well-known PTI inducer, can induce ROS production and transcriptional responses and provide protection against subsequent pathogen infection proving the existing PTI in sorghum (Kimball et al. 2019; Tuleski et al. 2020; Cui et al. 2021). Multiple NLRs, which are generally associated with ETI, have been identified as defense-related genes in sorghum. For instance, a leucine-rich repeat receptor kinase called DS1 showed a strong correlation with sorghum's resistance to target leaf spot caused by *Bipolaris sorghicola* infection (Kawahigashi et al. 2011). Recently, anthracnose resistance gene 1 (ARG1) and ARG2, two NLR proteins, were connected with sorghum broad-spectrum fungal resistance and defense against race-specific *Colletotrichum sublineola* strains (Lee et al. 2022; Mewa et al. 2022). Our study also suggested the existence of ETI in sorghum, as overexpressing HopAJ2 and HopAN1 reduced the pathogenicity of *Pss* van Hall. However, the HR was accompanied by HopAJ2- and HopAN1 in *N. benthamiana* but not in sorghum. We assume these two

(See figure on next page.)

**Fig. 5** Identification of *Pss* van Hall effectors that inhibit PTI in *N. benthamiana*. Leaves of five-week-old *N. benthamiana* were infiltrated with *Pst* DC3000 D36E harboring the pPSE vector with GFP or different *Pss* van Hall effectors. Samples were collected 6 h later for RNA extraction and then qPCR using the PTI marker genes **a** *Pti5* and **b** *ACRE31*, with *ACTIN* as an endogenous control. CK, samples without infection. Data are shown as the mean  $\pm$  SD (n = 3). **c** ROS production was performed at 15 h post-inoculation using L-012. Data are shown as the mean  $\pm$  SD (n = 8). **d** The bacterial population was measured at 4 days post-infiltration. Data are shown as the mean  $\pm$  SD (n = 8). All experiments were repeated three times with similar results. Significant differences were detected using Student's *t* test. \*  $p < 0.05$ ; \*\*  $p < 0.01$ ; \*\*\*  $p < 0.001$ ; \*\*\*\*  $p < 0.0001$

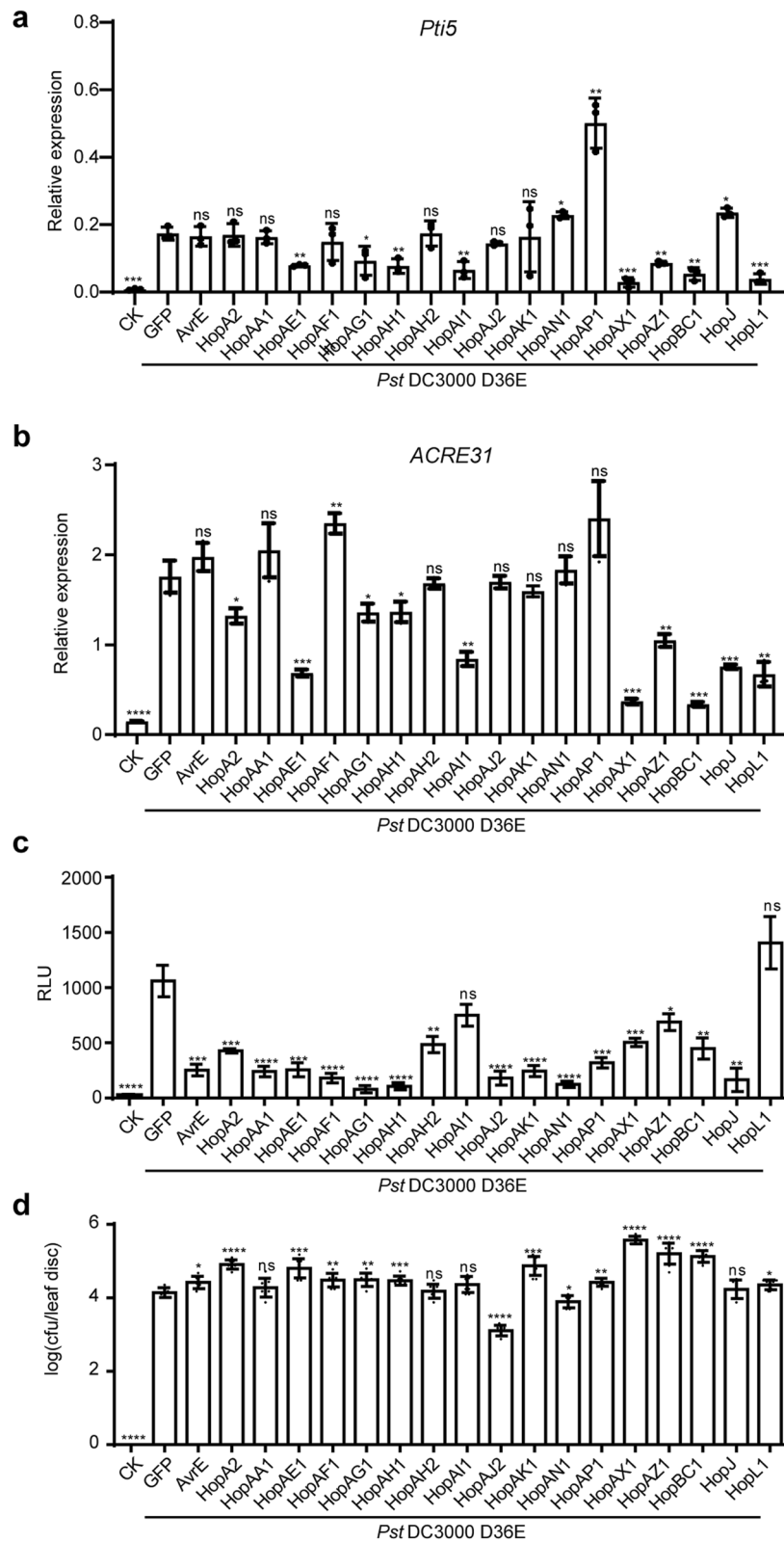


**Fig. 5** (See legend on previous page.)

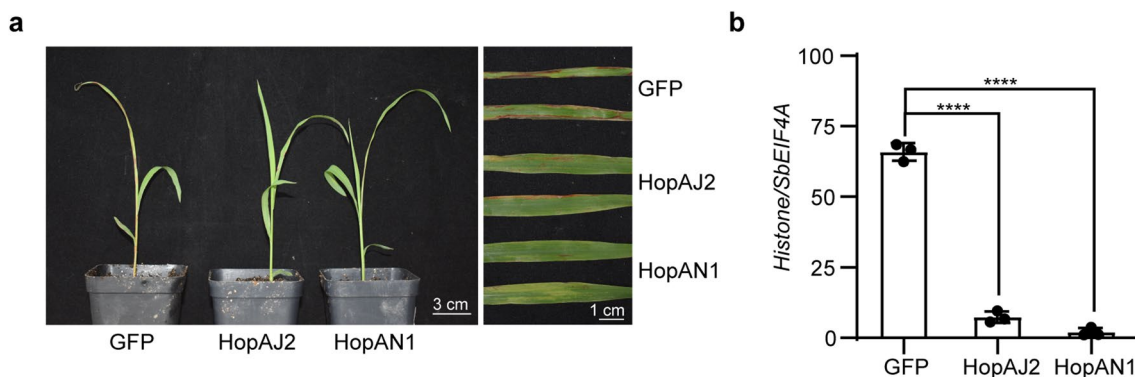


**Fig. 6** The functions of HopAJ2 and HopAN1 on the pathogenicity of *Pss van Hall* to sorghum. **a** Representative seedling and leaves of sorghum infected with *Pss van Hall* harboring the pPSE vector (GFP) or pPSE with *HopAJ2* or *HopAN1*. Two-week-old sorghum were treated with representative seedlings and leaves of sorghum infected with *Pss van Hall* harboring the pPSE vector (GFP) or pPSE with *HopAJ2* or *HopAN1* for 2 days at 12 °C and then kept at 25 °C for an additional 3 days. **b** The DNA level of the pathogen *Histone* gene, which is normalized to the DNA level of the sorghum gene *SbEIF4A*. Data are shown as the mean  $\pm$  SD ( $n=3$ ). All experiments were repeated three times with similar results. Significant differences were detected using Student's *t* test. \*\*\*\*  $p < 0.0001$

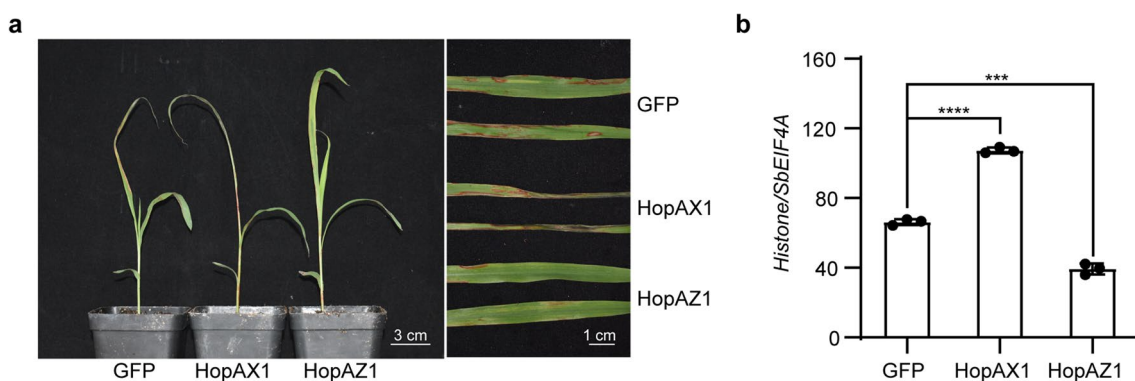


**Fig. 7** The functions of HopAX1 and HopAZ1 on the pathogenicity of *Pss van Hall* to sorghum. **a** Representative seedling and leaves of sorghum infected with *Pss van Hall* harboring the pPSE vector (GFP) or pPSE with *HopAX1* or *HopAZ1*. Two-week-old sorghum were treated with representative seedlings and leaves of sorghum infected with *Pss van Hall* harboring the pPSE vector (GFP) or pPSE with *HopAX1* or *HopAZ1* for 2 days at 12 °C and then kept at 25 °C for an additional 3 days. **b** The DNA level of the pathogen *Histone* gene, which is normalized to the DNA level of the sorghum gene *SbEIF4A*. Data are shown as the mean  $\pm$  SD ( $n=3$ ). All experiments were repeated three times with similar results. Significant differences were detected using Student's *t* test. \*\*\*  $p < 0.001$ ; \*\*\*\*  $p < 0.0001$

effectors are not HR-inducer or their functions might be repressed by other effectors of *Pss van Hall* in sorghum. Further exploration of the proteins required for HopAJ2- and HopAN1-triggered pathogen growth inhibition may be able to identify essential ETI components of sorghum.

The *Arabidopsis-Pseudomonas syringae* pathosystem has been extensively studied as a model to elucidate the signaling pathways of PTI and ETI over the past three decades (Quirino and Bent 2003; Ngou et al. 2022). However, it is important to note that *Arabidopsis* is a dicotyledonous plant, while sorghum is a monocotyledonous plant, and their immune-related components may not be entirely identical. *Pss van Hall*, a pathovar of

*P. syringae*, is a bacterial pathogen known to cause bacterial leaf spot disease in sorghum (Anitha et al. 2020), yet no study regarding the interaction between *Pss van Hall* and sorghum has been reported. Here, we established the *Pss van Hall*-sorghum pathosystem, provided whole genome information on *Pss van Hall*, and identified several *Pss van Hall* effectors that differentially modulate the sorghum immune response. Based on our results, we assume that *Pss van Hall* could serve as a valuable model for exploring the components of the sorghum immune system in the future.

A significant portion of our understanding of the plant immune system is gained from investigating the function

of *P. syringae* effectors (Xin and He 2013; Bundalovic-Torma et al. 2022). In this study, 18 effectors were predicted in *Pss* van Hall. The homologous proteins of several *Pss* van Hall effectors have been studied in other bacterial strains. For example, AvrE superfamily is widespread type III effectors, which could inhibit the plant immune response by modulating salicylic acid signaling and PTI (Jacobs et al. 2013; Degraeve et al. 2015). In addition, the AvrE from *Pst* DC3000 elicit cell death in *N. benthamiana* leaves (Badel et al. 2006; Wei et al. 2018). In our study, the expression of AvrE of *Pss* van Hall did not produce a distinct HR phenotype which might be due to the low homology between AvrEs from *Pss* van Hall and *Pst* DC3000 (Fig. 4b). HopAI1 from *Pst* DC3000 can dephosphorylate MPK3 and MPK6 proteins to suppress the PTI response (Zhang et al. 2007; Wang et al. 2010). HopAF1 from *Pph* 1448A can inhibit plant immunity by blocking ethylene induction by targeting methionine recycling, whose homology also promoted pathogenicity of *Pst* DC3000 D36E in our study (Washington et al. 2016). These effectors may cooperate with HopAX1 to suppress sorghum immunity during *Pss* van Hall infection. HopAJ2, HopAN1, and HopAX1 exhibited conserved roles in sorghum and *N. benthamiana*, and the functions of HopAN1 and HopAX1 have never been reported previously. Further exploration of how HopAN1 and HopAX1 regulate plant immunity may not only benefit sorghum but also help identify new plant immune components in general.

## Conclusions

In this study, we sequenced the whole genome of *Pss* van Hall. By analyzing the roles of its effectors in the *Pss* van Hall-plant interaction, we found its core effectors HopAJ2 and HopAN1 and the specific effector HopAX1 differently regulate the pathogenicity of *Pss* van Hall in sorghum. Notably, the small genome, facile sorghum infection, and identified ETI induction and immune inhibition effectors make *Pss* van Hall an ideal pathogen to investigate sorghum immunity. Further exploration of how these effectors regulate the sorghum defense response will identify resistance genes and provide a theoretical basis for the molecular breeding of sorghum disease-resistant varieties.

## Methods

### Bacterial strains and plant materials

The bacterial strains *Pss* van Hall and *Pst* DC3000 D36E were used in this study. *Sorghum bicolor* Btx623 and *N. benthamiana* plants were grown in a greenhouse at 25 °C with a 12/12 h light/dark cycle and 50–70% relative humidity before infection.

### *Pss* van Hall infection assay

*Pss* van Hall stock at –80 °C was streaked on KB (10 g proteose peptone, 1.5 g K<sub>2</sub>HPO<sub>4</sub>, 15 g glycerol, and 5 mL 1 M MgSO<sub>4</sub> in 1 L medium) agar medium and cultured at 28 °C for 2 days. Several colonies of *Pss* van Hall were then transferred to KB liquid medium and incubated at 28 °C overnight with shaking at 220 rpm. The bacteria were collected by centrifuging at 2500 g for 5 min and resuspended in solution containing 10 mM MgSO<sub>4</sub> and 0.04% Silwet L-77, with the concentration adjusted to OD<sub>600</sub>=0.6. The resuspended solution was evenly sprayed onto the leaf surface of 2-week-old sorghum seedlings. The treated materials were placed in a growth chamber at 12 °C and 65% humidity with a 16-h light/8-h dark cycle for 2 days. Subsequently, they were transferred to a greenhouse at 25 °C for an additional 3 days to observe the infection status.

Genomic DNA was extracted from the infected leaves using CTAB buffer (0.1 M Tris-HCl (pH 8.0), 0.02 M EDTA (pH 8.0), 81.9 g/L NaCl, 20 g/L CTAB, and 20 g/L polyvinylpyrrolidone), and the DNA concentration was subsequently diluted to 5.5 µg/µL. qPCR was performed to evaluate the level of *Pss* van Hall *Histone* with sorghum *SbEIF4A* as a control.

### HR assay in *N. benthamiana*

*Pss* van Hall and *Pst* DC3000 D36E expressing GFP or different *Pss* van Hall effectors were grown in KB liquid medium at 28 °C overnight with shaking at 200 rpm. Then, the bacterial pellet was resuspended in 10 mM MgSO<sub>4</sub> solution with the concentration adjusted to OD<sub>600</sub>=0.01 for *Pss* van Hall and OD<sub>600</sub>=0.6 for others. The bacterial suspension was infiltrated into leaves of 5-week-old *N. benthamiana* plants using a syringe. Photographs were taken 2 days later.

Ion leakage measurement was performed as described previously with little modification (Wang and Balint-Kurti 2016; Wang et al. 2023). Briefly, leaf discs were punched from infiltrated *N. benthamiana* leaves and transferred to 10 mL centrifuge tubes with 3 mL ddH<sub>2</sub>O. The tubes with samples were then shaken at 150 rpm at 28 °C for 3 h. Subsequently, the conductivity (C1) was measured using a conductivity meter. The samples were further boiled for 15 min and allowed to cool to room temperature to measure the total conductivity (C2). The ratio of C1/C2 was used to represent the ion leakage of the corresponding sample.

### Genome sequencing of *Pss* van Hall and its bioinformatics analysis

*Pss* van Hall was grown in 100 mL of KB liquid medium at 28 °C overnight with shaking at 200 rpm. The bacterial cells were then collected by centrifugation at 2500 g

for 5 min, and the pellet was washed 3 times with sterile water and frozen in liquid nitrogen. The frozen cells were subsequently sent to Wuhan Bioacme Biological Technology Company for genome sequencing using Illumina HiSeq technology and third-generation sequencing technologies.

After sequencing, the raw data underwent quality trimming by removing the low-quality reads. The assembled sequences were statistically analyzed using QUAST (Gurevich et al. 2013), and Prokka (Seemann 2014) was employed for structural annotation. KEGG analysis was performed using the public database (<http://www.genome.jp/kegg/>).

#### Plasmid construction

To extract *Pss* van Hall DNA for cloning effector genes, a single colony of *Pss* van Hall was diluted in 10  $\mu$ L ddH<sub>2</sub>O and heated at 95 °C for 10 min. The sample was then frozen at -80 °C for 5 min and centrifuged at 13,500 *g* for 5 min to remove the cell debris. The *Pss* van Hall DNA in the supernatant was used as a template for gene amplification. To generate constructs for the expression of effector genes, full-length coding sequences of effectors were amplified and inserted into the *Sall*- and *Xho*I-digested pPSE plasmid using homologous recombination. The primers for amplifying effector genes are listed in Additional file 2: Table S2.

#### Generation of the $\Delta$ *hrpL* mutant

To generate the  $\Delta$ *hrpL* mutant, fragments of upstream and downstream sequences (200 bp each) of the *hrpL* gene were amplified. These fragments, along with the expression cassette of the gentamicin resistance gene in the middle, were inserted into the pENTR<sup>TM</sup>/SD/D-TOPO<sup>TM</sup> vectors (Thermo Fisher) using the ClonExpress MultiS One Step Cloning Kit (Vazyme). Then, a fragment of the *hrpL* upstream sequence-gentamycin expression cassette-*hrpL* downstream sequence was amplified (Liu et al. 2022). The PCR product was purified and introduced into *Pss* van Hall competent cells that expressed homologous recombination enzymes for selecting knock-out mutants on KB solid medium supplemented with 50 mg/L gentamicin.

#### The transformation of *P. syringae*

To prepare the competent cells of *P. syringae*, the overnight culture was centrifuged, and the pellet was resuspended in precooled 10% glycerol and centrifuged at 3000 *g* for 5 min. This process was repeated three times, and the final pellet was resuspended in 1 ml 10% glycerol, which was the competent cell solution.

For transformation, 1  $\mu$ g plasmid containing effector genes or DNA fragments for gene knockout was mixed

with 100  $\mu$ L competent cell solution. The mixture was transferred into a precooled electroporation cuvette and kept on ice for 15 min. Set an electroporator at specific parameters (1800 V, 200  $\Omega$ , and 25  $\mu$ F) for electroporation. After electroporation, the bacteria were incubated in KB liquid medium at 28 °C with shaking at 220 rpm for 2 h before being placed on selection medium.

#### Western blot

For western blots, overnight cultures of *Pst* DC3000 D36E or *Pss* van Hall harboring different *Pss* van Hall effectors were centrifuged, and the pellet was resuspended in 150  $\mu$ L PBS (137 mM NaCl, 2.7 mM KCl, 10 mM Na<sub>2</sub>HPO<sub>4</sub>, 2 mM KH<sub>2</sub>PO<sub>4</sub>) buffer. Next, 50  $\mu$ L of 4 $\times$ protein loading buffer (0.3125 M TrisHCl (pH 6.8), 10% SDS, 50% glycerol, 0.005% bromophenol blue, 25% 2-mercaptoethanol) was added, and the mixture was boiled at 100 °C for 10 min, followed by centrifugation at 4 °C for 15 min. The resulting supernatant was used for western blotting using an anti-Flag antibody (EASYBIO, BE2004) (Liu et al. 2022).

#### qPCR

Total RNA was extracted from *N. benthamiana* leaves using TRIzol reagent (Takara). Then, cDNA was synthesized using MixHiScript III RT SuperMix (Vazyme), and qPCR was performed using SYBR Green mix (Mei5Bio), with *Actin* as an internal control. The primers used for qPCR are listed in Additional file 2: Table S2.

#### Assays for effector translocation

For the effector translocation assay, the coding sequence of flag tag of the pPSE-effector constructs was replaced by the coding sequence of Cya. Then, the effector-Cya expressing vectors were introduced into *Pst* DC3000 D36E through electroporation. The transformed bacteria were resuspended in 10 mM MgSO<sub>4</sub> with an OD<sub>600</sub>=0.6 and infiltrated into leaves of *N. benthamiana*. The leaf discs of *N. benthamiana* were collected 6 h later. The cAMP levels were determined using a direct cAMP ELISA kit according to the manufacturer's instructions (ADI-901-066, Enzo, USA) (Cong et al. 2023).

#### ROS assay

For ROS measurement, bacteria were resuspended in 10 mM MgSO<sub>4</sub> with an OD<sub>600</sub>=0.6 and infiltrated into *N. benthamiana* leaves. After 15 h inoculation, the leaf discs were excised and placed into wells of 96-well plates with 100  $\mu$ L ddH<sub>2</sub>O. Before measurement using a 96-well microplate luminometer (BERTHOLD, Centro XS LB 960), 100  $\mu$ L 0.5 mM L-012 (Wako, Japan) in 10 mM

morpholinepropanesulfonic acid-KOH buffer (pH 7.4) was added to each well (Wei et al. 2018).

### Bacterial growth

*Pst* DC3000 D36E harboring different *Pss* van Hall effector were streaked onto KB medium containing 50 µg/mL kanamycin and grown in a 28 °C incubator for 36 h. These bacteria were resuspended in 10 mM MgSO<sub>4</sub> with an OD<sub>600</sub> = 0.004 and infiltrated into the leaves of *N. benthamiana*. Four days later, 16 leaf discs were surface sterilized and then randomly divided into 8 sample pools for bacterial growth measurement according to a previously reported method (Yuan et al. 2021; Liu et al. 2023).

### Determination of bacterial growth curve

To determine whether overexpression of HopAN1, HopAJ2, HopAX1, and HopAZ1 affects the growth of *Pss* van Hall, 300 µL bacterial solution (OD<sub>600</sub> = 1.0) was added into 30 mL fresh KB liquid culture medium. The bacterial suspension was then cultured in a 28 °C incubator with an agitation speed of 200 rpm. To monitor the growth, the absorbance of the cell suspension at 600 nm was measured every 3 h for 24 h using a UV-visible spectrophotometer (Jiang et al. 2022).

### Abbreviations

<i>Pss</i> van Hall	<i>Pseudomonas syringae syringae</i> van Hall
HR	Hypersensitive response
ETI	Effector-triggered immunity
PTI	Pattern-triggered immunity
PAMPs	Pathogen-associated molecular patterns
PRRs	Pattern recognition receptors
ETS	Effector-triggered susceptibility
NLRs	Nucleotide-binding domain leucine-rich repeat-containing receptors
T3SS	Type III secretion system
CDS	Coding sequences
KEGG	Kyoto Encyclopedia of Genes and Genomes
ARG1	Anthrax resistance gene 1
RBS	Ribosome-binding site
Cya	C-terminal calmodulin-dependent adenylate cyclase

### Supplementary Information

The online version contains supplementary material available at <https://doi.org/10.1186/s42483-023-00218-5>.

**Additional file 1: Figure S1.** The establishment of sorghum-*Pss* van Hall and *N. benthamiana*-*Pss* van Hall pathosystems. **Figure S2.** The DNA gel showing CDSs of all 18 *Pss* van Hall effectors cloned using PCR. **Figure S3.** The pPSE vector is an effective vector to express functional *Pseudomonas* effectors. **Figure S4.** The levels of all 18 *Pss* van Hall effectors expressed in *Pst* DC3000 D36E. **Figure S5.** The levels of effectors HopAN1, HopAJ2, HopAX1, and HopAZ1 expressed in *Pss* van Hall. **Figure S6.** Overexpression of HopAJ2, HopAN1, HopAX1, and HopAZ1 does not affect the growth of *Pss* van Hall in medium.

**Additional file 2: Table S1.** Type III effectors in the *Pss* van Hall genome. **Table S2.** The primers used in this study.

### Acknowledgements

We thank Youming Zhang from State Key Laboratory of Microbial Technology, Shandong University, China, for sharing the vector that expressed homologous recombination enzymes; Xiufang Xin from Institute of Plant Physiology and Ecology, Chinese Academy of Sciences, China, for sharing the *Pst* DC3000 D36E; and Mingyi Bai from Shandong University, China, for sharing the pENTR<sup>TM</sup>/SD/D-TOPO<sup>TM</sup> vectors.

### Author contributions

FY, XW, and LL designed the experiments. FY, XW, GM, and AL performed the experiments. FY and XW provided the resources and analyzed the data. LL wrote the manuscript. All authors read and approved the final manuscript.

### Funding

This work was supported by the National Natural Science Foundation of China (No. 32101685 for Aixia Li and 32000224 for Lijing Liu).

### Availability of data and materials

The data that support the findings of this study are available from the corresponding author upon reasonable request. The genome sequence of *Pss* van Hall have submitted to NCBI (the accession number is SUB13931676).

### Declarations

#### Ethics approval and consent to participate

Not applicable.

#### Consent for publication

Not applicable.

#### Competing interests

The authors declare that they have no competing interests.

Received: 1 July 2023 Accepted: 18 November 2023

Published online: 22 December 2023

### References

- Ackerman A, Wennndt A, Boyles R. The sorghum grain mold disease complex: pathogens, host responses, and the bioactive metabolites at play. *Front Plant Sci.* 2021;12:660171.
- Alfano JR, Bauer DW, Milos TM, Collmer A. Analysis of the role of the *Pseudomonas syringae* pv. *syringae* HrpZ harpin in elicitation of the hypersensitive response in tobacco using functionally non-polar hrpZ deletion mutations, truncated HrpZ fragments, and hrmA mutations. *Mol Microbiol.* 1996;19:715–28.
- Anitha K, Das IK, Holajjer P, Sivaraj N, Reddy CR, Balijepalli SB. Sorghum diseases: diagnosis and management. Singapore: Springer; 2020.
- Badel JL, Shimizu R, Oh HS, Collmer A. A *Pseudomonas syringae* pv. tomato avrE1/hopM1 mutant is severely reduced in growth and lesion formation in tomato. *Mol Plant Microbe Interact.* 2006;19:99–111.
- Bundalovic-Torma C, Lonjon F, Desveaux D, Guttman DS. Diversity, evolution, and function of *Pseudomonas syringae* effectoromes. *Annu Rev Phytopathol.* 2022;60:211–36.
- Calvino M, Messing J. Sweet sorghum as a model system for bioenergy crops. *Curr Opin Biotech.* 2012;23:323–9.
- Chinchilla D, Bauer Z, Regenass M, Boller T, Felix G. The Arabidopsis receptor kinase FLS2 binds flg22 and determines the specificity of flagellin perception. *Plant Cell.* 2006;18:465–76.
- Clark K, Franco JY, Schwizer S, Pang Z, Hawara E, Liebrand TWH, et al. An effector from the Huanglongbing-associated pathogen targets citrus proteases. *Nat Commun.* 2018;9:1718.
- Colombini S, Galassi G, Crovetto GM, Rapetti L. Milk production, nitrogen balance, and fiber digestibility prediction of corn, whole plant grain sorghum, and forage sorghum silages in the dairy cow. *J Dairy Sci.* 2012;95:4457–67.

- Cong S, Li JZ, Xiong ZZ, Wei HL. Diverse interactions of five core type III effectors from *Ralstonia solanacearum* with plants. *J Genet Genomics*. 2023;50:341–52.
- Cui Y, Chen D, Jiang Y, Xu D, Balint-Kurti P, Stacey G. Variation in gene expression between two sorghum bicolor lines differing in innate immunity response. *Plants Basel*. 2021;10:1536.
- Degrave A, Siamer S, Boureau T, Barny MA. The AvrE superfamily: ancestral type III effectors involved in suppression of pathogen-associated molecular pattern-triggered immunity. *Mol Plant Pathol*. 2015;16:899–905.
- Dillon SL, Shapter FM, Henry RJ, Cordeiro G, Izquierdo L, Lee LS. Domestication to crop improvement: genetic resources for Sorghum and saccharum (Andropogoneae). *Ann Bot Lond*. 2007;100:975–89.
- Donati I, Cellini A, Buriani G, Mauri S, Kay C, Tacconi G, et al. Pathways of flower infection and pollen-mediated dispersion of *Pseudomonas syringae* pv. actinidiae, the causal agent of kiwifruit bacterial canker. *Hortic Res*. 2018;5:56.
- Gassmann W, Bhattacharjee S. Effector-triggered immunity signaling: from gene-for-gene pathways to protein–protein interaction networks. *Mol Plant Microbe Interact*. 2012;25:862–8.
- Gurevich A, Saveliev V, Vyahhi N, Tesler G. QUASt: quality assessment tool for genome assemblies. *Bioinformatics*. 2013;29:1072–5.
- Ivanovic Z, Perovic T, Popovic T, Blagojevic J, Trkulja N, Hrcic S. Characterization of *Pseudomonas syringae* pv. *syringae*, causal agent of citrus blast of mandarin in Montenegro. *Plant Pathol J*. 2017;33:21–33.
- Jacobs JM, Milling A, Mitra RM, Hogan CS, Ailloud F, Prior P, et al. *Ralstonia solanacearum* requires PopS, an ancient AvrE-family effector, for virulence and To overcome salicylic acid-mediated defenses during tomato pathogenesis. *mBio*. 2013;4:e00875-13.
- Jiang L, Xiang S, Lv X, Wang X, Li F, Liu W, et al. Biosynthesized silver nanoparticles inhibit *Pseudomonas syringae* pv. *tabaci* by directly destroying bacteria and inducing plant resistance in *Nicotiana benthamiana*. *Phytopathol Res*. 2022;4:43.
- Jones JD, Dangl JL. The plant immune system. *Nature*. 2006;444:323–9.
- Kawahigashi H, Kasuga S, Ando T, Kanamori H, Wu J, Yonemaru J, et al. Positional cloning of *ds1*, the target leaf spot resistance gene against *Bipolaris sorghicola* in sorghum. *Theor Appl Genet*. 2011;123:131–42.
- Khoddami A, Messina V, Vadabalija Venkata K, Farahnaky A, Blanchard CL, Roberts TH. Sorghum in foods: functionality and potential in innovative products. *Crit Rev Food Sci Nutr*. 2021; 1–17.
- Kimball J, Cui Y, Chen D, Brown P, Rooney WL, Stacey G, et al. Identification of QTL for target leaf spot resistance in Sorghum bicolor and investigation of relationships between disease resistance and variation in the MAMP response. *Sci Rep*. 2019;9:18285.
- Kunkel BN, Bent AF, Dahlbeck D, Innes RW, Staskawicz BJ. RPS2, an Arabidopsis disease resistance locus specifying recognition of *Pseudomonas syringae* strains expressing the avirulence gene *avrRpt2*. *Plant Cell*. 1993;5:865–75.
- Kunze G, Zipfel C, Robatzek S, Niehaus K, Boller T, Felix G. The N terminus of bacterial elongation factor Tu elicits innate immunity in Arabidopsis plants. *Plant Cell*. 2004;16:3496–507.
- Lee S, Fu F, Liao CJ, Mewa DB, Adeyanju A, Ejeta G, et al. Broad-spectrum fungal resistance in sorghum is conferred through the complex regulation of an immune receptor gene embedded in a natural antisense transcript. *Plant Cell*. 2022;34:1641–65.
- Liu N, Lian S, Li B, Ren W. The autophagy protein BcAtg2 regulates growth, development and pathogenicity in the gray mold fungus *Botrytis cinerea*. *Phytopathol Res*. 2022;4:1–8.
- Liu L, Sonbol FM, Huot B, Gu Y, Withers J, Mwimba M, et al. Salicylic acid receptors activate jasmonic acid signalling through a non-canonical pathway to promote effector-triggered immunity. *Nat Commun*. 2016;7:13099.
- Liu Y, Gong T, Kong X, Sun J, Liu L. XYLEM CYSTEINE PEPTIDASE 1 and its inhibitor CYSTATIN 6 regulate pattern-triggered immunity by modulating the stability of the NADPH oxidase RBOHD. *Plant Cell*. 2023.
- Ma S, Lv L, Meng C, Zhang C, Li Y. Integrative analysis of the metabolome and transcriptome of sorghum bicolor reveals dynamic changes in flavonoids accumulation under saline-alkali stress. *J Agric Food Chem*. 2020;68:14781–9.
- Matas IM, Castaneda-Ojeda MP, Aragon IM, Antunez-Lamas M, Murillo J, Rodriguez-Palenzuela P, et al. Translocation and functional analysis of *Pseudomonas savastanoi* pv. *savastanoi* NCPPB 3335 type III secretion system effectors reveals two novel effector families of the *Pseudomonas syringae* complex. *Mol Plant Microbe Interact*. 2014;27:424–36.
- Mewa DB, Lee S, Liao CJ, Adeyanju A, Helm M, Lisch D, et al. ANTHRACNOSE RESISTANCE GENE2 confers fungal resistance in sorghum. *Plant J*. 2022.
- Ngou BPM, Ding PT, Jones JDG. Thirty years of resistance: zig-zag through the plant immune system. *Plant Cell*. 2022;34:1447–78.
- Paterson AH, Bowers JE, Bruggmann R, Dubchak I, Grimwood J, Gundlach H, et al. The *Sorghum bicolor* genome and the diversification of grasses. *Nature*. 2009;457:551–6.
- Prasad VBR, Govindaraj M, Djanaguiraman M, Djalovic I, Shailani A, Rawat N, et al. Drought and high temperature stress in sorghum: physiological, genetic, and molecular insights and breeding approaches. *Int J Mol Sci*. 2021;22:9826.
- Qi Y, Li J, Mapuranga J, Zhang N, Chang J, Shen Q, et al. Wheat leaf rust fungus effector Pt13024 is avirulent to TcLR30. *Front Plant Sci*. 2022;13:1098549.
- Quirino BF, Bent AF. Deciphering host resistance and pathogen virulence: the *Arabidopsis/Pseudomonas* interaction as a model. *Mol Plant Pathol*. 2003;4:517–30.
- Ravindran A, Jalan N, Yuan JS, Wang N, Gross DC. Comparative genomics of *Pseudomonas syringae* pv. *syringae* strains B301D and H5191 and insights into intrapathovar traits associated with plant pathogenesis. *Microbiol Biogeochem*. 2015;4:553–73.
- Rooney WL, Blumenthal J, Bean B, Mullet JE. Designing sorghum as a dedicated bioenergy feedstock. *Biofuel Bioprod Bior*. 2007;1:147–57.
- Seemann T. Prokka: rapid prokaryotic genome annotation. *Bioinformatics*. 2014;30:2068–9.
- Stothard P, Grant JR, Van Domselaar G. Visualizing and comparing circular genomes using the CGView family of tools. *Brief Bioinform*. 2019;20:1576–82.
- Studholme DJ, Ibanez SG, MacLean D, Dangl JL, Chang JH, Rathjen JP. A draft genome sequence and functional screen reveals the repertoire of type III secreted proteins of *Pseudomonas syringae* pathovar *tabaci* 11528. *BMC Genomics*. 2009;10:395.
- Sun X, Li A, Ma G, Zhao S, Liu L. Transcriptome analysis provides insights into the bases of salicylic acid-induced resistance to anthracnose in sorghum. *Plant Mol Biol*. 2022;110:69–80.
- Tang X, Xiao Y, Zhou JM. Regulation of the type III secretion system in phytopathogenic bacteria. *Mol Plant Microbe Interact*. 2006;19:1159–66.
- Todd JNA, Carreon-Anguiano KG, Islas-Flores I, Canto-Canche B. Microbial effectors: key determinants in plant health and disease. *Microorganisms*. 2022;10:1980.
- Tuleski TR, Kimball J, do Amaral FP, Pereira TP, Tadra-Sfeir MZ, de Oliveira Pedrosa F, et al. *Herbaspirillum rubrisubalbicans* as a phytopathogenic model to study the immune system of sorghum bicolor. *Mol Plant Microbe Interact*. 2020;33:235–46.
- Wang GF, Balint-Kurti PJ. Maize homologs of CCoAOMT and HCT, two key enzymes in lignin biosynthesis, form complexes with the NLR Rp1 protein to modulate the defense response. *Plant Physiol*. 2016;171:2166–77.
- Wang Y, Li J, Hou S, Wang X, Li Y, Ren D, et al. A *Pseudomonas syringae* ADP-ribosyltransferase inhibits Arabidopsis mitogen-activated protein kinase kinases. *Plant Cell*. 2010;22:2033–44.
- Wang S, Yang S, Dai K, Zheng W, Zhang X, Yang B, et al. The effector Fg62 contributes to *Fusarium graminearum* virulence and induces plant cell death. *Phytopathology Research*. 2023;5:12.
- Washington EJ, Mukhtar MS, Finkel OM, Wan L, Banfield MJ, Kieber JJ, et al. *Pseudomonas syringae* type III effector HopAF1 suppresses plant immunity by targeting methionine recycling to block ethylene induction. *Proc Natl Acad Sci USA*. 2016;113:E3577–86.
- Wei HL, Zhang W, Collmer A. Modular study of the type III effector repertoire in *Pseudomonas syringae* pv. *tomato* DC3000 reveals a matrix of effector interplay in pathogenesis. *Cell Rep*. 2018;23:1630–8.
- White FF, Yang B, Johnson LB. Prospects for understanding avirulence gene function. *Curr Opin Plant Biol*. 2000;3:291–8.
- Xie Q, Xu Z. Sustainable agriculture: from sweet sorghum planting and ensiling to ruminant feeding. *Mol Plant*. 2019;12:603–6.
- Xin XF, He SY. *Pseudomonas syringae* pv. *tomato* DC3000: a model pathogen for probing disease susceptibility and hormone signaling in plants. *Annu Rev Phytopathol*. 2013;51:473–98.
- Xin XF, Kvitko B, He SY. *Pseudomonas syringae*: what it takes to be a pathogen. *Nat Rev Microbiol*. 2018;16:316–28.
- Yuan M, Jiang Z, Bi G, Nomura K, Liu M, Wang Y, et al. Pattern-recognition receptors are required for NLR-mediated plant immunity. *Nature*. 2021;592:105–9.

Zhang J, Shao F, Li Y, Cui H, Chen L, Li H, et al. A *Pseudomonas syringae* effector inactivates MAPKs to suppress PAMP-induced immunity in plants. *Cell Host Microbe*. 2007;1:175–85.

**Ready to submit your research? Choose BMC and benefit from:**

- fast, convenient online submission
- thorough peer review by experienced researchers in your field
- rapid publication on acceptance
- support for research data, including large and complex data types
- gold Open Access which fosters wider collaboration and increased citations
- maximum visibility for your research: over 100M website views per year

**At BMC, research is always in progress.**

Learn more [biomedcentral.com/submissions](https://biomedcentral.com/submissions)

